Nuclear Theory'21
ed. V. Nikolaev, Heron Press, Sofia, 2002

Current Issues in Electromagnetic Knockout Reactions

C. Giusti

Dipartimento di Fisica Nucleare e Teorica, Università di Pavia, Istituto Nazionale di Fisica Nucleare, Sezione di Pavia, Pavia, Italy

Abstract.

The role of correlations and two-body currents in one-nucleon emission reactions induced by an electromagnetic probe is discussed. The theoretical framework for cross section calculations is outlined and some results are presented for the exclusive ^{16}O$(e,e'p)^{15}$N and ^{16}O$(\gamma,p)^{15}$N reactions in relativistic and nonrelativistic models. A reliable and consistent evaluation of different types of correlations is needed to determine the spectroscopic factors. A consistent description of $(e,e'p)$ and (γ,p) data, with the same spectroscopic factors, can be obtained when meson-exchange currents (MEC) are included in the theoretical model. MEC give an important contribution to (γ,p) cross sections and have only a small effect in $(e,e'p)$. In the relativistic model the two-body seagull current affects the calculated cross sections less than in the nonrelativistic calculations.

1 Introduction

Electromagnetically induced one-nucleon knockout reactions are powerful tools to explore the conditions of individual nucleons in the nuclear medium. Several measurements at different energies and kinematics have been performed in a wide range of target nuclei, which stimulated the production of a considerable amount of theoretical work. [1].

For an exclusive reaction, the coincidence cross section contains the one-hole spectral density function, i.e.

$$S(\boldsymbol{p}_1,\boldsymbol{p}'_1;E_{\rm m}) = \langle\Psi_{\rm i}|a^+_{\boldsymbol{p}'_1}\delta(E_{\rm m}-H)a_{\boldsymbol{p}_1}|\Psi_{\rm i}\rangle, \qquad (1)$$

which in its diagonal form ($\boldsymbol{p}_1 = \boldsymbol{p}'_1$) gives the joint probability of removing from the target a nucleon, with momentum $\boldsymbol{p}_1$, leaving the residual nucleus in a

state with energy $E_{\rm m}$ with respect to the target ground state. In an inclusive reaction, integrating the spectral density over the whole energy spectrum produces the one-body density matrix (OBDM) $\rho(\boldsymbol{p}_1, \boldsymbol{p}'_1)$, that in its diagonal form gives the nucleon momentum distribution $n(\boldsymbol{p}_1)$.

The spectral function contains information on NN correlations. In order to extract this information, however, along with the experimental work, a reliable theoretical model for cross section calculations is needed, able to keep under control the reaction mechanism and all the theoretical ingredients contributing to the cross section. In particular, a careful evaluation of all the correlations contained in the spectral density function is necessary. Thus, a reliable calculation must include the short-range correlations (SRC), produced by the short-range components of the NN interaction, as well as the tensor correlations (TC), which are induced by the strong tensor components of the interaction and which mainly originate from the pion exchange contributions. Moreover, it is necessary to consider also those processes beyond the mean-field (MF) approximation falling under the generic name of long-range correlations (LRC), which are related to the coupling between the single-particle (s.p.) dynamics and the collective excitation modes of the nucleus. These processes mainly represent the interaction of nucleons at the nuclear surface and can be very important in finite nuclear systems. Various theoretical methods have been developed to account for such correlation effects (see, e.g., [2–4]).

The quasifree $(e, e'p)$ reaction has extensively been used to investigate the s.p. properties of nuclei and to point out the validity and the limit of the independent-particle shell model (IPSM) [1]. For exclusive processes the direct knockout (DKO) mechanism is clearly established. Different theoretical models based on the nonrelativistic and relativistic distorted wave impulse approximation (DWIA) are able to give an excellent description of the shape but generally overestimate the size of the experimental angular distributions [1]. The fact that a pure MF picture is unable to give a precise quantitative description of $(e, e'p)$ data is an indication of the relevance of correlations and the discrepancy can give a measurement of their effects. The same information is in principle available from the (γ, p) reaction. The reaction mechanism of photonucleon emission, however, is more questionable and has been the object of a longstanding debate. Important effects are expected in (γ, p) from two-body mechanisms such as those involving two-body currents [1].

In this contribution the role of correlations and two-body currents in exclusive $(e, e'p)$ and (γ, p) reactions is reviewed. The $(e, e'p)$ knockout reaction is discussed in Section 2. The effects of two-body currents in nonrelativistic and relativistic frameworks are investigated in Section 3 and in Section 4, respectively.

2 One-Nucleon Knockout

2.1 The Plane-Wave Impulse Approximation

In the one-photon exchange approximation, where the incident electron exchanges a photon of momentum $\boldsymbol{q}$ and energy ω with the target, the most general form of the coincidence $(e, e'N)$ cross section involves the contraction between a lepton tensor $L_{\mu\nu}$ and a hadron tensor $W^{\mu\nu}$. The lepton tensor is produced by the matrix elements of the electron current and, neglecting the effect of the nuclear Coulomb field on electrons, contains only electron kinematics. The components of the hadron tensor are given by bilinear combinations of the Fourier transforms of the transition matrix elements of the nuclear current operator between initial and final nuclear states, i.e.

$$J^{\mu}(\boldsymbol{q}) = \int \langle \Psi_{\rm f} | \hat{J}^{\mu}(\boldsymbol{r}) | \Psi_{\rm i} \rangle \mathrm{e}^{\,\mathrm{i}\boldsymbol{q}\cdot\boldsymbol{r}} \mathrm{d}\boldsymbol{r}. \tag{2}$$

In the plane-wave impulse approximation (PWIA), i.e. neglecting the final-state interactions (FSI) of the ejected particle with the residual nucleus, the $(e, e'p)$ cross section is factorized as a product of a kinematical factor, the (off-shell) electron-proton cross section and, for an exclusive reaction, the one-hole diagonal spectral density function

$$S(\boldsymbol{p}_{\rm m}, E_{\rm m}) = \sum_{\alpha} S_{\alpha}(E_{\rm m}) |\phi_{\alpha}(\boldsymbol{p}_{\rm m})|^2, \tag{3}$$

where the missing momentum $\boldsymbol{p}_{\rm m}$ is the recoil momentum of the residual nucleus. At each value of $E_{\rm m}$, the momentum dependence of the spectral function is given by the momentum distribution of the quasi-hole (q.h.) states α produced in the target nucleus at that energy and described by the normalized overlap functions (OF) ϕ_{α} between the target ground state and the states of the residual nucleus. The (normalization) spectroscopic factor (s.f.) S_{α} gives the probability that the q.h. state α is a pure hole-state in the target. In an IPSM ϕ_{α} are the s.p. states of the model and $S_{\alpha} = 1(0)$ for occupied (empty) states. In reality, the strength of a q.h. state is fragmented over a set of s.p. states, and $0 \leq S_{\alpha} \leq 1$. The fragmentation of the strength is due to correlations and the s.f. can thus give a measurement of correlation effects.

The PWIA is a simple and clear picture that is able to describe the main qualitative features of $(e, e'p)$ cross sections, but is unable to give a precise quantitative description of data. For the analysis of data a more refined theoretical treatment is needed. The calculations for this analysis were carried out with the program DWEEPY [5], within the theoretical framework of a nonrelativistic DWIA, where FSI and Coulomb distortion of the electron wave functions are taken into account.

2.2 The Distorted-Wave Impulse Approximation

The DWIA treatment of the matrix elements in Eq. (2) is based on the following assumptions :
i) An exclusive process is considered, where the residual nucleus is left in a discrete eigenstate $|\Psi^{\rm B}_{\alpha}(E)\rangle$ of its Hamiltonian, with energy E and quantum numbers α.
ii) The final nuclear state is projected onto the channel subspace spanned by the vectors corresponding to a nucleon, at $\boldsymbol{r}_1$, and the residual nucleus in the state $|\Psi^{\rm B}_{\alpha}(E)\rangle$. This assumption neglects effects of coupled channels and is justified by the considered asymptotic configuration of the final state.
iii) The (one-body) nuclear-current operator does not connect different channel subspaces. Thus, also the initial state is projected onto the selected channel subspace. This assumption is the basis of the DKO mechanism and is related to the IA.

The transition matrix elements in Eq. (2) can thus be written in a one-body representation as

$$J^{\mu}(\boldsymbol{q}) = \int \chi^{(-)*}_{E\alpha}(\boldsymbol{r}_1)\hat{J}^{\mu}(\boldsymbol{r},\boldsymbol{r}_1)\phi_{E\alpha}(\boldsymbol{r}_1)\left[S_{\alpha}(E)\right]^{1/2}{\rm e}^{\,{\rm i}\boldsymbol{q}\cdot\boldsymbol{r}}{\rm d}\boldsymbol{r}{\rm d}\boldsymbol{r}_1, \quad (4)$$

where

$$\chi^{(-)}_{E\alpha}(\boldsymbol{r}_1) = \langle\Psi^{\rm B}_{\alpha}(E)|a_{\boldsymbol{r}_1}|\Psi_{\rm f}\rangle \quad (5)$$

is the s.p. distorted wave function of the ejectile and the overlap function

$$\left[S_{\alpha}(E)\right]^{1/2}\phi_{E\alpha}(\boldsymbol{r}_1) = \langle\Psi^{\rm B}_{\alpha}(E)|a_{\boldsymbol{r}_1}|\Psi_{\rm i}\rangle \quad (6)$$

describes the residual nucleus as a hole state in the target. The spectroscopic strength $S_{\alpha}(E)$ is the norm of the overlap integral in the right-hand side of Eq. (6) and gives the probability of removing from the target a nucleon at $\boldsymbol{r}_1$ leaving the residual nucleus in the state $\Psi^{\rm B}_{\alpha}(E,\boldsymbol{r}_1)$.

The scattering state in Eq. (5) and the bound state $\phi_{E\alpha}(\boldsymbol{r}_1)$ in Eq. (6) are consistently derived in this model from an energy-dependent non-Hermitean optical model Feshbach Hamiltonian. In standard DWIA calculations, however, phenomenological ingredients are employed. The nucleon scattering state is eigenfunction of a phenomenological optical potential, determined through a fit to elastic nucleon-nucleus scattering data including cross sections and polarizations. Phenomenological bound-state wave functions are usually adopted for the OF, which thus do not include correlations. In the analysis of data these functions were calculated in a Woods-Saxon well, where the radius was determined to fit the experimental momentum distributions and the depth was adjusted to reproduce the experimentally observed separation energy of the bound final state. In order to reproduce the magnitude of the experimental cross sections, a reduction

factor was applied to the calculated results. This factor was then identified with the s.f.

The "experimental" spectroscopic factors extracted in these DWIA analyses indicate that the removal of the s.p. strength for q.h. states near the Fermi energy is about 60-70%. The s.f. gives a measurement of correlation effects, but, since in these $(e, e'p)$ analyses it is obtained through a fit to the data, it can include, besides correlations, also other contributions which are neglected or not adequately described by the model. It can be correctly identified with the s.f. only if all the theoretical ingredients contributing to the cross sections are reasonably under control. On the other hand, the fact that this model, with phenomenological ingredients, was able to give an excellent description of $(e, e'p)$ data, in a wide range of nuclei and in different kinematics (see, e.g., [1, 6]), gives support and consistency to this whole picture and to the interpretation of the s.f. extracted in comparison with data in terms of correlations.

2.3 Overlap Functions and Correlations

Explicit calculations of the hole spectral function and the associated fully correlated OF for complex nuclei are very difficult. Only recently the first successful parameter-free comparison of experiment and theory including the absolute normalization in p-shell nuclei has been performed for the ^{7}Li$(e, e'p)$ reaction [7]. For heavier nuclei a calculation able to account for the effects due to all types of correlations appears extremely difficult, since it requires excessively large model space.

Correlation effects have been investigated within several theoretical frameworks and with different approximations. The effects of a spectral function containing only SRC and TC [8] and only LRC [9] have been investigated in the ^{16}O$(e, e'p)$ reaction. The one-body density matrix, momentum distribution, natural orbits and q.h. states of ^{16}O and ^{40}Ca have been analyzed in the framework of the correlated basis function (CBF) theory using state-dependent correlations with central and tensor components [10]. The contribution of SRC in ^{16}O$(e, e'p)$ has been also studied [11]. Methods to deal with SRC and LRC consistently have been proposed and applied to ^{16}O in refs. [12, 13], where, however, only the s.f. and not the OF have been calculated.

Recently, a general procedure has been adopted [14] to extract the OF and the associated s.f. on the base of the OBDM. The advantage of this procedure is that it avoids the complicated task of calculating the nuclear spectral function, but its success depends on the availability of realistic calculations of the OBDM. This procedure has been applied [15–19] to OBDM of ^{16}O and ^{40}Ca constructed within different correlation methods. The OF and the s.f. have then been used to calculate the cross section of one-nucleon removal reactions [17–19].

The result of all this theoretical work is that only a few percent of the depletion of the q.h. states is due to SRC. When TC are added to SRC the depletion

amounts to $\sim 10\%$, at most $\sim 15\%$ in heavy nuclei. Further depletion is given by LRC. A full and consistent calculation of the OF and of the s.f. including all types of correlations is not yet available and in all these analyses at least a part of the contribution of correlations is obtained in terms of a reduction factor in comparison with data.

Two examples are displayed in Figures 1 and 2 for the ^{16}O$(e, e'p)$ reaction. The results are presented in terms of the reduced cross section [1], which is defined as the cross section divided by a kinematical factor and the elementary off-shell electron-proton scattering cross section. In PWIA the reduced cross section gives the momentum distribution of the q.h. state. The experimental data were taken in the so-called parallel kinematics, where the momentum of the outgoing nucleon is fixed and is taken parallel or antiparallel to the momentum transfer. Different values of $\boldsymbol{p}_{\rm m}$ are obtained by varying the electron scattering angle and therefore the magnitude of the momentum transfer. The calculations have been performed with same code DWEEPY [5] used in the original analysis of the NIKHEF data [26], in the same conditions and with the same optical potential [20], but the phenomenological s.p. bound state wave functions have been replaced by different theoretically calculated OF. For the results in Figure 1 the OF are extracted in [18] from the asymptotic behaviour of OBDM constructed within different correlation methods, such as the Jastrow correlation method (JCM) [15], the CBF theory [22, 23], the Green's function method (GFM) [21], and the generator coordinate method (GCM) [24, 25]. The reduced cross sections in Figure 2 are obtained with the OF calculated in [10] in the framework of the CBF theory. In the figure the results given by q.h. states where only Jastrow correlations (JAS) and Jastrow, spin-isospin (SI) and TC correlations are included are shown and compared with the results obtained with an IPSM wave function.

The q.h. wave functions contain the s.f. listed in column I of Table 1. They account, however, only for the contribution of the correlations included in the model. In order to reproduce the size of the experimental cross section, a reduction factor has been applied in Figures 1 and 2 to the calculated results. These factors are also listed in Table 1 (column II). They can be considered as further s.f. reflecting the depletion of the q.h. state produced by the correlations not included in the model. The product of the two factors, in column III, can thus be considered as the total s.f. accounting for the combined effect of all the correlations. For the two transitions, the same values are obtained for the three q.h. states of ref. [10]. These values are in reasonable agreement with the values given by the OF extracted from the different calculations of the OBDM and for $1p_{1/2}$ in agreement with the s.f. (0.77) obtained in the calculation of ref. [12, 13]. The fact that for $1p_{3/2}$ the s.f. in column III are lower than the those found in [12] and [13] (0.76 and 0.72) is presumably due to the approximations used in those calculations and requires a more sophisticated treatment of LRC.

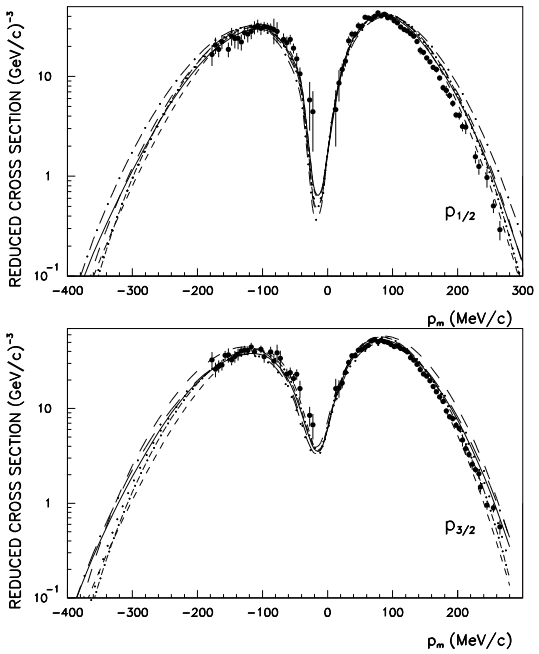

Figure 1. Reduced cross sections of the ^{16}O$(e, e'p)$ reaction as a function of the missing momentum $p_{\rm m}$ for the transitions to the $1/2^-$ ground state and to the first $3/2^-$ excited state of ^{15}N in parallel kinematics, with an incident electron energy $E_0 = 520.6$ MeV and an outgoing proton energy $T_1' = 90$ MeV. The optical potential is taken from ref. [20]. The OF are derived from the OBDM of GFM [21] (solid line), CBF [22] (long-dashed line), CBF [23] (long-dot-dashed line), JCM [15] (short-dot-dashed line), and GCM [25] (short-dashed line). The dotted line is calculated with the HF wave function. The positive (negative) values of $p_{\rm m}$ refer to situations where $|\boldsymbol{q}| < |\boldsymbol{p}'|$ ($|\boldsymbol{q}| > |\boldsymbol{p}'|$). The experimental data are taken from ref. [26]. The theoretical results have been multiplied by the reduction factor given in column II of Table 1 (from ref. [18]).

In Figure 1 the calculated reduced cross sections are sensitive to the shape of the various OF, where correlations are included within different theoretical frameworks. It is interesting to notice that the best agreement with data, for both transitions, is obtained with the OF emerging from the OBDM calculated within the GFM [21] and corresponding to the most refined calculation of the OBDM. The differences given by the different OF are larger at large values of $p_{\rm m}$, where correlation effects are more sizable. On the contrary, the curves in Figure 2 are insensitive to the shape of the different wave functions, which include different types of correlations within the same theoretical framework. Only very slight differences are found at the highest values of $p_{\rm m}$ shown in the figure. Thus, at least in the considered region of momenta, the shape of the OF is practically unaffected

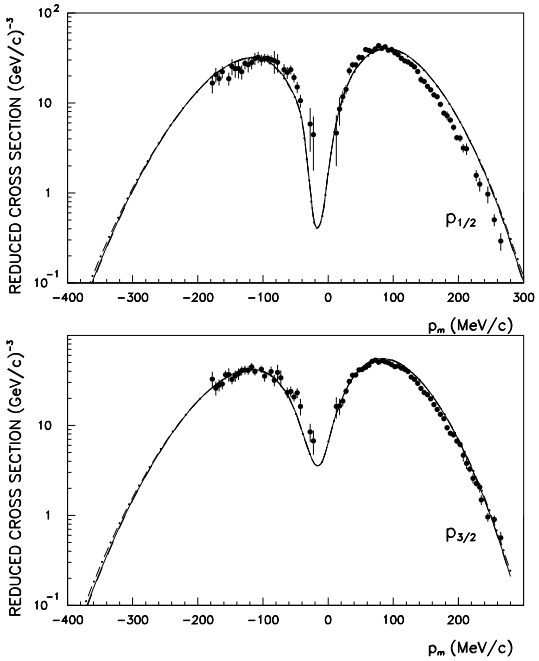

Figure 2. The same as in Figure 1 but with the q.h. wave functions from ref. [10]: JAS+SI+TC (solid lines); JAS (dashed lines); IPSM (dot-dashed lines).

by the correlations included in the q.h. wave functions. Correlations affect only the norm, i.e. the s.f.

3 Meson-Exchange Currents in Photonucleon Emission

DWIA calculations for the ^{16}O$(\gamma, p)^{15}$N$_{\rm g.s.}$ reaction at $E_\gamma = 60$ MeV are displayed in the left panel of Figure 3 [18]. The results given by the OF extracted from the different calculations of the OBDM are shown in the figure. In order to allow a consistent comparison of $(e, e'p)$ and (γ, p) results, the reduction factors listed in column II of Table 1 and determined through a fit to $(e, e'p)$ data have been applied to the calculated cross sections. A different kinematical situation is explored in photon-induced reactions. In fact, for a real photon the energy and momentum transfer are constrained by the condition $\omega = |\boldsymbol{q}| = E_\gamma$, and only the high-momentum components of the nuclear wave function are probed, higher values than in the usual kinematics of $(e, e'p)$ experiments. Thus, it is not strange that the differences given by the different OF are so large, in particular at backward angles, which correspond to higher values of $p_{\rm m}$. The agreement of the DWIA calculations with data is anyhow poor.

For the (γ, p) reaction the validity of the DKO mechanism related to the

Table 1. Spectroscopic factors for the ^{16}O$(e,e'p)$ knockout reaction leading to the $1/2^-$ ground state and to the $3/2^-$ excited state of ^{15}N. Column I gives the s.f. obtained from the calculations of the different OF; II gives the reduction factors determined through a comparison between the $(e,e'p)$ data of ref. [26] and the reduced cross sections calculated in DWIA with the different OF; III gives the total s.f. obtained from the product of the factors in columns I and II.

	$1p_{1/2}$			$1p_{3/2}$		
OF	I	II	III	I	II	III
HF	1.000	0.750	0.750	1.000	0.550	0.550
JCM [15]	0.953	0.825	0.786	0.953	0.600	0.572
CBF [22]	0.912	0.850	0.775	0.909	0.780	0.709
CBF [23]	0.981	0.900	0.883	0.981	0.600	0.589
GFM [21]	0.905	0.800	0.724	0.915	0.625	0.572
GCM [24]	0.988	0.700	0.692	0.988	0.500	0.494
SM [10]	1.000	0.770	0.770	1.000	0.570	0.570
JAS [10]	0.980	0.786	0.770	0.980	0.580	0.570
JAS+SI+TC [10]	0.900	0.860	0.770	0.900	0.630	0.570

DWIA, which is clearly stated for $(e,e'p)$, is questionable and large contributions are expected by two-nucleon processes, such as those involving two-body meson-exchange currents (MEC). Indeed a better agreement with data is obtained in the right panel of Figure 3, where MEC are added to the DKO contribution. Here MEC have been included within the theoretical framework of ref. [30], in a microscopic and unfactorized calculation. In the transition matrix elements the nuclear current is given by the sum of a one-body part, corresponding to the DKO contribution, and of a two-body part, corresponding to the reaction process where the interaction occurs with a pair of nucleons: one of them is emitted and the other nucleon is reabsorbed in the residual nucleus. For the nucleon which is not emitted a sum over all the s.p. states is performed. This makes the numerical calculations technically difficult and time consuming. In order to reduce the complexity of the calculation, some approximation have been made [18, 30]. The spin-orbit part of the optical potential has been neglected and only the contribution due to the seagull diagrams with one-pion exchange is included.

In Figure 3 the seagull current produces a significant enhancement of the cross section which brings the results closer to data. The differences for the various OF are however still large and for some functions the agreement with data remains poor. The best agreement and a fair description of data is given by the OF from GFM [21], which is able to give also the best description of $(e,e'p)$ data and with the same s.f. This result, that has been confirmed also in different situations [18], is a strong indication in favour of a consistent description of the two reactions.

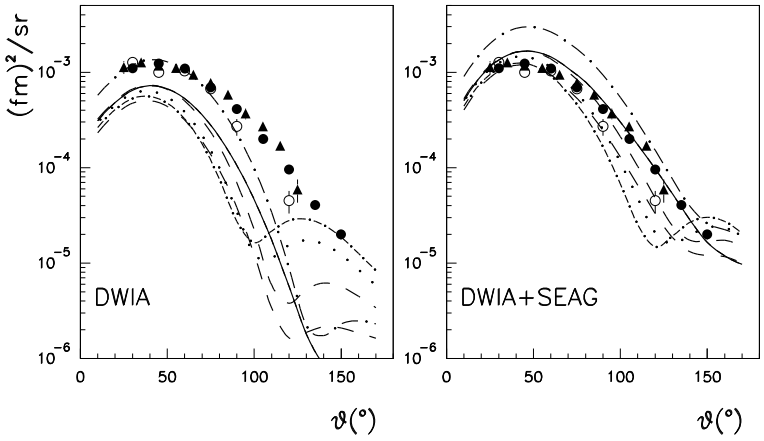

Figure 3. Angular distributions of the ^{16}O$(\gamma, p)^{15}$N$_{\rm g.s.}$ reaction at $E_\gamma = 60$ MeV. The separate contribution given by the one-body current (DWIA) and the final result given by the sum of the one-body and the two-body seagull current (DWIA+SEAG) are shown. Line convention as in Figure 1. The optical potential is taken from ref. [20]. The experimental data are taken from refs. [27] (black circles), [28] (open circles) and [29] (triangles). The theoretical results have been multiplied by the reduction factors extracted in ref. [18] in comparison with $(e, e'p)$ data (from ref. [18]).

The seagull current, however, gives only a part of the contribution of MEC. A more careful evaluation requires to add at least the other terms due to the exchange of one pion, namely the pion-in-flight and the Δ-current. It has been shown in a recent paper [31] that the contribution of these terms can be important and the use of only the seagull current overestimates the MEC effects.

The theoretical approach of ref. [30] has been improved [32]. A new numerical code has just been written, where also the pion-in-flight and the Δ contributions are added in the two-body current and also the spin-orbit term is included in the optical potential. Some first results are presented in Figures 4 and 5.

The cross sections of the ^{16}O(γ, p) reaction at $E_\gamma = 60$ MeV are shown in Figure 4. Calculations have been performed with the wave function from GFM [21], able to give a consistent description of $(e, e'p)$ and (γ, p) data in Figures 1 and 3. The results in Figure 4 show that MEC effects are overestimated by the seagull term. A significant reduction is obtained when the pion-in-flight term is added, while the Δ-current is not very important at the considered value of the photon energy. The MEC contribution remains anyhow large and important to improve the agreement with data. As a consequence of the reduction produced by the pion-in-flight current, the experimental cross section for the transition to the ground state, which is already well reproduced when only the seagull term is included in the two-body current, is somewhat underestimated, while a better

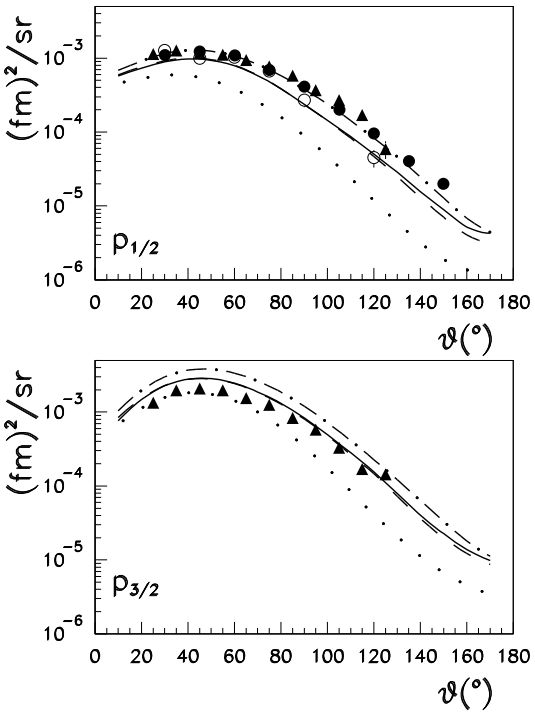

Figure 4. Angular distributions of the ^{16}O(γ, p) reaction for the transitions to the $1/2^-$ ground state and to the first $3/2^-$ excited state of ^{15}N at $E_\gamma = 60$ MeV. The OF are derived from the OBDM of GFM [21] and the optical potential is taken from ref. [20]. Experimental data as in Figure 3. The dotted lines give the contribution of the one-body current (DWIA). The other lines have been obtained by adding the various terms of the two-body current: one-body + seagull (dot-dashed lines), one-body + seagull + pion-in-flight (dashed lines), one-body+ seagull+ pion-in-flight+ Δ (solid lines). The theoretical results have been multiplied by the reduction factors extracted in ref. [18] in comparison with ($e, e'p$) data.

agreement with data is found for the transition to the $3/2^-$ state.

The cross sections of the ^{16}O(γ, p)^{15}N$_{\rm g.s.}$ reaction at $E_\gamma = 100$ and 196 MeV are shown in Figure 5. The contribution of the two-body current is always large. Important effects are given by the pion-in-flight and, at 196 MeV, also by the Δ-current. A good agreement with data is achieved at 100 MeV when the pion-in flight term is added. At 196 MeV a good agreement with data is obtained, when the Δ-current is added, for nucleon emission angles up to $\sim 70^{\rm o}$, while for larger angles the enhancement produced by the two-body current, in particular by the pion-in-flight term, overestimates the experimental cross section. In this region, however, recoil-momentum values around 700-800 MeV/c are probed,

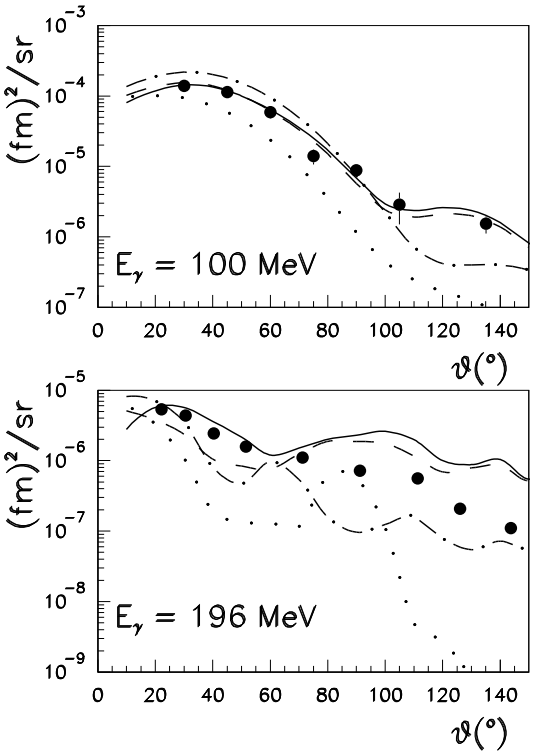

Figure 5. Angular distributions of the ^{16}O$(\gamma,p)^{15}$N$_{\rm g.s.}$ reaction at $E_\gamma = 100$ and 196 MeV. OF and line convention as in Figure 4. The optical potential is taken from ref. [20]. The experimental data are taken from ref. [27] ($E_\gamma = 100$) and ref. [33] ($E_\gamma = 196$). The theoretical results have been multiplied by the reduction factor extracted in ref. [18] in comparison with $(e,e'p)$ data.

where the behaviour of the wave function may become critical and also the role of correlations, which becomes more important increasing the photon energy and the outgoing nucleon angle [30, 31], should more carefully be considered.

The calculated cross sections are very sensitive to details of the model and to the theoretical ingredients of the calculation. For instance, the contribution of the one-body current and its interference with the different terms of the two-body current are sensitive to the choice of the bound state wave function. The present results anyhow indicate that MEC give an important contribution to (γ,p) cross sections at all the considered photon energies. All the pion-exchange diagrams must be included in the model. In contrast, the $(e,e'p)$ cross sections are practically unaffected by two-body currents [32, 34]. A reasonable and consistent description of $(e,e'p)$ and (γ,p) data is obtained, with a consistent choice of the

theoretical ingredients and with the same s.f., for recoil momentum values up to $\sim 500 - 600$ MeV/c.

This result gives further support to the $(e, e'p)$ analyses, where the contribution to the depletion of the q.h. states produced by the different types of correlations has been established. A part of this contribution, however, is still obtained as a reduction factor in comparison with data. Thus, also in this analyses, the s.f. can be affected by other effects not included or not adequately decribed in the theoretical model.

4 Relativistic Effects

Various contributions and their effect on the extracted s.f. have been studied in recent years. A proper treatment of the c.m. motion leads to an enhancement of the extracted s.f. by about 7% [35]. A further enhancement is obtained in relativistic DWIA (RDWIA) analyses with relativistic optical potentials [36, 37].

Fully relativistic models based on the RDWIA have been developed by different groups in recent years [36, 38]. In these approaches the bound nucleons are described by s.p. Dirac wave functions in the presence of scalar and vector potentials fitted to the ground-state properties of the nucleus, and the scattering wave function is solution of the Dirac equation with relativistic optical potentials obtained by fitting elastic proton-nucleus scattering data. Also RDWIA analyses are able to give a good description of $(e, e'p)$ data. RDWIA calculations are necessary for the analyses of the new $(e, e'p)$ data from Jlab [39] in kinematic conditions inaccessible in previous experiments, where the four-momentum transfer squared Q^2 was less than 0.4 (GeV/c)^2 and the outgoing proton energy generally around 100 MeV. It is anyhow important to check the relevance of relativistic effects also in the kinematics at lower energies of the previous experiments, whose data were analyzed with a nonrelativistic DWIA treatment.

Relativistic effects as well as the differences between relativistic and nonrelativistic calculations have been investigated in different papers where RDWIA treatments have been developed. The differences, however, are usually evaluated starting from the basis of a relativistic model where terms corresponding to relativistic effects are cancelled or where nonrelativistic approximations are included. Although very interesting, these investigations do not correspond to the result of a comparison between RDWIA and the DWIA calculations carried out with the program DWEEPY. In fact, DWEEPY is based on a nonrelativistic treatment where some relativistic corrections are introduced in the kinematics and in the nuclear current operator. On the other hand, only indirect comparison between relativistic and nonrelativistic calculations can be obtained from the available data analyses carried out with DWEEPY and in RDWIA. In fact, the two types of calculations make generally use of different optical potentials and bound state wave functions, and the difference due to the different theoretical ingredients cannot be attributed to relativity.

In order to investigate the relevance of genuine relativistic effects through a direct comparison between RDWIA calculations and the results of DWEEPY, a fully relativistic RDWIA model for the $(e, e'p)$ reaction has been developed and its numerical results have been compared with the corresponding results given by DWEEPY [38]. In order to make the comparison as consistent as possible, in the nonrelativistic calculations the bound state is the normalized upper component of the Dirac spinor and the scattering state is the solution of the same Schrödinger-equivalent optical potential of the relativistic calculation. This is not the best choice for DWEEPY, but the same theoretical ingredients are to be used for a clear comparison between the two approaches.

An example is shown in Figure 6, for the ^{16}O$(e, e'p)$ reaction in comparison with the NIKHEF data [26]. Only small differences are found between the two calculations in this kinematics. The reduction (spectroscopic) factor applied to the calculated reduced cross sections in order to reproduce the size of the experimental results is 0.7 for RDWIA and 0.65 for DWIA, for both the transitions, which confirms that somewhat higher spectroscopic factors are obtained in RDWIA.

The systematic investigation carried out in ref. [38] indicates that relativistic effects increase with the energy and in particular with the energy of the outgoing proton. The DWIA approach can be used with enough confidence at the energies around 100 MeV of previous $(e, e'p)$ experiments, and, with some caution, up to about 200 MeV. This confirms the validity of the analyses carried out with DWEEPY at lower energies. A fully relativistic calculation is anyhow convenient at 200 MeV and necessary above 300 MeV. Thus, RDWIA must be used in comparison with the recent data from JLab [39], at Q^2 = 0.8 (GeV/c)^2 and $T'_1 = 433$ Mev. Here the RDWIA model gives an excellent description of data keeping the same spectroscopic factor (0.7) extracted in the comparison with the NIKHEF data of Figure 6 [38].

The comparison between the RDWIA and DWIA results is shown in Figure 7 for the cross section of the ^{16}O$(\gamma, p)^{15}$N$_{\rm g.s.}$ reaction in a photon-energy range between 60 MeV and 257 MeV [42]. The nonrelativistic calculations are not extended above 200 MeV. For the relativistic calculations results obtained with different expressions of the one-body current operator are compared. In fact, the choice of the operator is, to some extent, arbitrary and an unambiguos approach to deal with off-shell nucleon is unavailable. The three most commonly used current-conserving (cc) prescriptions [44] are here considered:

$$\begin{aligned} j^{\mu}_{\rm cc1} =& G_M(Q^2)\gamma^{\mu} - \frac{\kappa}{2M}F_2(Q^2)\overline{P}^{\mu} \ , \\ j^{\mu}_{\rm cc2} =& F_1(Q^2)\gamma^{\mu} + i\frac{\kappa}{2M}F_2(Q^2)\sigma^{\mu\nu}q_{\nu} \ , \\ j^{\mu}_{\rm cc3} =& F_1(Q^2)\frac{\overline{P}^{\mu}}{2M} + \frac{i}{2M}G_M(Q^2)\sigma^{\mu\nu}q_{\nu} \ , \end{aligned} \tag{7}$$

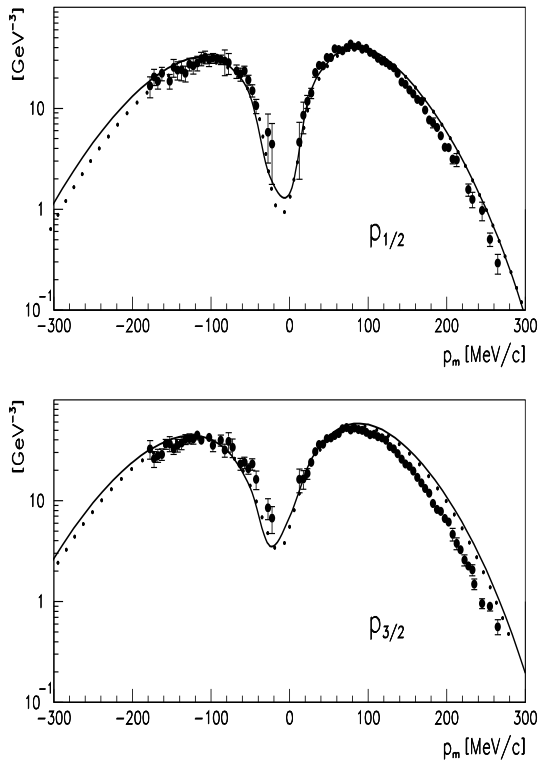

Figure 6. Reduced cross sections of the ^{16}O$(e,e'p)$ reaction as a function of the missing momentum $p_{\rm m}$ for the transitions to the $1/2^-$ ground state and to the first $3/2^-$ excited state of ^{15}N in the same kinematics as in Figure 1. The solid lines give the RDWIA result [38] the dotted lines the nonrelativistic result. The optical potential is taken from ref. [40] and the bound state wave functions from ref. [41] (from ref. [38]).

where $\overline{P}^{\mu} = (E+E', \boldsymbol{p}_{\rm m}+\boldsymbol{p}')$, κ is the anomalous part of the magnetic moment, F_1 and F_2 are the Dirac and Pauli nucleon form factors, $G_M = F_1 + \kappa F_2$ is the Sachs nucleon magnetic form factor, and $\sigma^{\mu\nu} = (i/2)\,[\gamma^{\mu}, \gamma^{\nu}]$. These expressions are equivalent for on-shell particles due to Gordon identity, but they give different results when applied to off-shell nucleons.

In $(e,e'p)$ the results of different prescriptions are generally in close agreement [45], but large differences can be found at high missing momenta [46, 47]. These differences increase in (γ,p) reactions, where the kinematics is deeply off-shell and higher values of the missing momentum are probed.

In Figure 7 the cc2 results are in satisfactory agreement with the experimental data at lower energies, but they tend to fall down with increasing proton angle and photon energy. RDWIA results are strongly enhanced with cc1. This is prob-

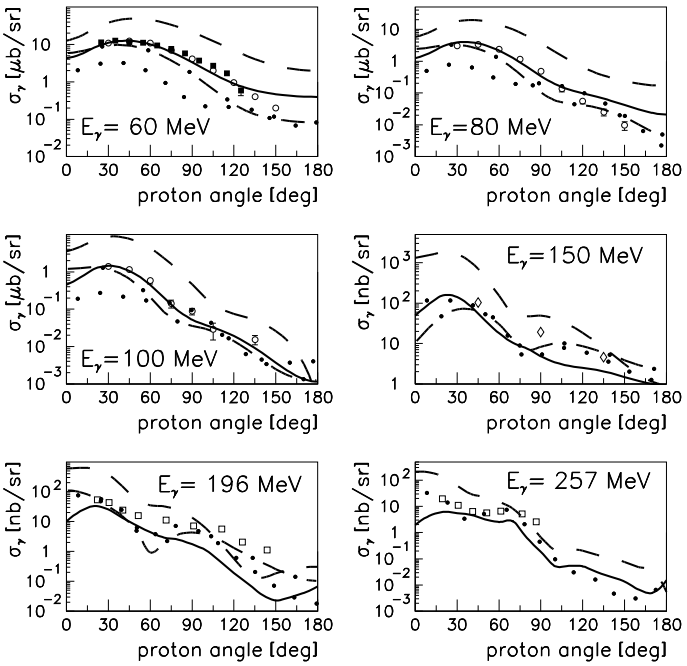

Figure 7. Angular distributions of the $^{16}\mathrm{O}(\gamma, p)^{15}\mathrm{N}_{\mathrm{g.s.}}$ reaction for photon energies ranging from 60 to 257 MeV. The data at 60 MeV are from ref. [29] (black squares) and from ref. [27] (open circles). The data at 80 and 100 MeV are from ref. [27]. The data at 150 MeV are from ref. [43], and those at 196 and 257 MeV from ref. [33]. The RDWIA results correspond to calculations with the cc2 (solid lines), cc1 (dashed lines), and cc3 (dotted lines) current. The dot-dashed lines are the nonrelativistic results. The optical potential is taken from ref. [40] and the bound state wave functions from ref. [41]. The theoretical results have been multiplied by the reduction factors extracted in ref. [38] in comparison with $(e, e'p)$ data (from ref. [42]).

ably due to a too small interference term which does not correctly estimate the convective current contained in both γ^μ and $\overline{P}^\mu/(2M)$ terms when the nucleon is off-shell. The results with cc3 are more similar to the cc2 ones. At low energy cc3 lies below cc2, but the differences rapidly decrease with the energy.

It is interesting to notice that the nonrelativistic reductions of the three cc forms give identical results up to order $1/M$. The nonrelativistic current is written as an expansion up to order $1/M^2$ from a Foldy-Wouthuysen transformation [48, 49] applied to the interaction Hamiltonian where the nuclear current is in the cc2 form. Thus, the cc2 prescription is more appropriate in the comparison between the relativistic and nonrelativistic models.

The differences between the DWIA and RDWIA calculations with the cc2

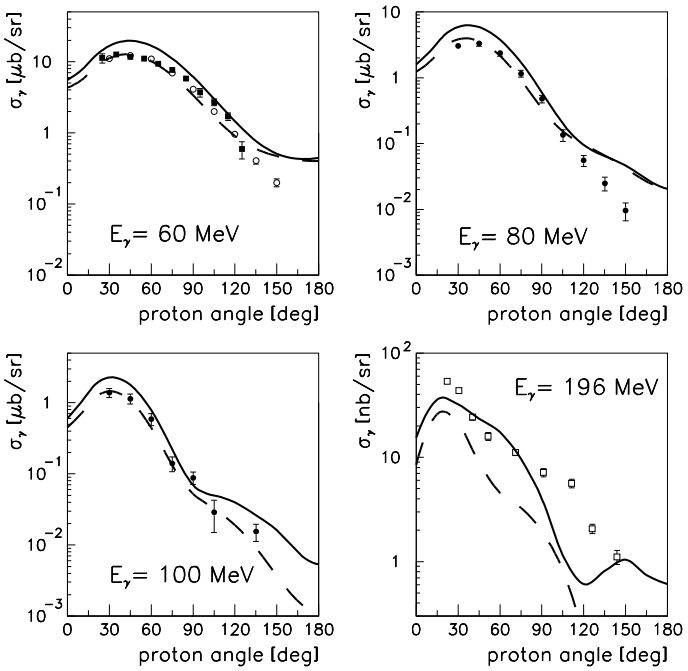

Figure 8. Angular distributions of the $^{16}\mathrm{O}(\gamma, p)^{15}\mathrm{N}_{\mathrm{g.s.}}$ reaction for photon energies ranging from 60 to 196 MeV. Experimental data, bound state wave functions and optical potential as in Figure 7. The dashed lines give the RDWIA results with the cc2 current, the solid lines the RDWIA+SEAG results. The calculated cross sections have been multiplied by the reduction factors extracted in ref. [38] in comparison with $(e, e'p)$ data.

prescription are sensible at all energies. The DWIA results are different from the corresponding results shown in Section 3. This is a further indication of the sensitivity of the calculated cross sections to the theoretical ingredients of the model (bound states and optical potentials). The DWIA results are anyhow always below the data. This result is not unexpected, since a significant enhancement is given by MEC in norelativistic calculations. On the contrary, the relativistic results are generally closer to the data and well reproduce the magnitude and shape, at least at low energies. This seems to indicate that in relativistic calculations the DKO mechanism gives the most important contribution to the cross section at lower missing momenta without the need to add MEC, while more complicated processes such as MEC and Δ-excitations become important at larger momenta.

A first step has been made to study the role of MEC in a fully relativistic framework [50]. Only the seagull current has been included in this first study. This contribution, however, should be able to understand the relevance of two-body currents in a relativistic approach also in comparison with the results of non-

relativistic calculations.

An example is shown in Figure 8, for the cross section of the $^{16}\mathrm{O}(\gamma, p)^{15}\mathrm{N}_{\mathrm{g.s.}}$ reaction in a photon-energy range between 60 MeV and 196 MeV. The seagull contribution enhances the cross section at all the considered photon energies, but less than in the nonrelativistic calculations. This is an indication that the role of two-body currents is less important in a relativistic approach. As a consequence of the enhancement produced by the seagull term, the experimental cross section up to $E_\gamma = 100$ MeV, that are already reproduced by the RDWIA results, are overestimated, while a better agreement with data is found at higher photon energies. In order to draw definite conclusions in comparison with data, however, it would be useful to check the relevance of the pion-in-flight contribution and also of the Δ-current, that should play a significant role above 150 MeV.

Acknowledgments

I want to thank all the colleagues and friends who contributed to this work, in particular F.D. Pacati, A. Meucci, A.N. Antonov, M.K. Gaidarov, G. Co' and A. Fabrocini.

References

[1] S. Boffi, C. Giusti, F.D. Pacati and M. Radici, (1996) *Electromagnetic Response of Atomic Nuclei* (Clarendon Press, Oxford).

[2] A.N. Antonov, P.E. Hodgson and I.Zh. Petkov, (1988) *Nucleon Momentum and Density Distributions in Nuclei* (Clarendon Press, Oxford).

[3] A.N. Antonov, P.E. Hodgson and I.Zh. Petkov, (1993) *Nucleon Correlations in Nuclei* (Springer–Verlag, Berlin).

[4] H. Müther and A. Polls, (2000) *Prog. Part. Nucl. Phys.* **45** 243.

[5] C. Giusti and F.D. Pacati, (1987) *Nucl. Phys.* **A473** 717; (1988) *Nucl. Phys.* **A485** 461.

[6] L. Lapikás, (1993) *Nucl. Phys.* **A553** 297c.

[7] L. Lapikás, J. Wesseling, and R.B. Wiringa, (1999) *Phys. Rev. Lett.* **82** 4404.

[8] A. Polls *et al.*, (1997) *Phys. Rev.* **C55** 810.

[9] K. Amir-Azimi-Nili, H. Müther, L.D. Skouras, and A. Polls, (1996) *Nucl. Phys.* **A604** 245;
K. Amir-Azimi-Nili *et al.*, (1997) *Nucl. Phys.* **A625** 633.

[10] A. Fabrocini and G. Co', (2001) *Phys. Rev.* **C63** 044319.

[11] S.R. Mokhtar, M. Anguiano, G. Co' and A.M. Lallena, (2001) *Annals Phys.* **293** 67.

[12] W.J.W. Geurts, K. Allaart, W.H. Dickhoff, and H. Müther, (1996) *Phys. Rev.* **C53** 2207.

[13] C. Barbieri and W.H Dickhoff, (2001) *Phys. Rev.* **C63** 034313; (2002) *Phys. Rev.* **C65** 064313.

[14] D. Van Neck, M. Waroquier, and K. Heyde, (1993) *Phys. Lett.* **B314** 255.

[15] M.V. Stoitsov, S.S. Dimitrova, and A.N. Antonov, (1996) *Phys. Rev.* **C53** 1254.

[16] S.S. Dimitrova *et al.*, (1997) *J. Phys.* **G23** 1685.

[17] M.K. Gaidarov *et al.*, (1999) *Phys. Rev.* **C60** 024312.

[18] M.K. Gaidarov *et al.*, (2000) *Phys. Rev.* **C61** 014306.

[19] M.V. Ivanov, M.K. Gaidarov, A.N. Antonov, and C. Giusti, (2001) *Phys. Rev.* **C64** 014605.

[20] P. Schwandt *et al.*, (1982) Phys. Rev. **C26** 55.

[21] A. Polls, H. Müther, and W.H. Dickhoff, (1995) *Proceedings of the Conference on Perspectives in Nuclear Physics at Intermediate Energies*, Trieste, (edited by S. Boffi, C. Ciofi degli Atti, and M.M. Giannini; World Scientific, Singapore,1996) p.308.

[22] D. Van Neck, L. Van Daele, Y. Dewulf, and M. Waroquier, (1997) *Phys. Rev.* **C56** 1398.

[23] F. Arias de Saavedra, G. Co', A. Fabrocini, and S. Fantoni, (1996) *Nucl. Phys.* **A605** 359.

[24] A.N. Antonov, Chr.V. Christov, and I.Zh. Petkov, (1986) *Nuovo Cim.* **91A** 119; A.N. Antonov, I.S. Bonev, Chr.V. Christov, and I.Zh. Petkov, (1988) *Nuovo Cim.* **100A** 779; A.N. Antonov, I.S. Bonev, and I.Zh. Petkov, (1991) *Bulg. J. Phys.* **18** 169; A.N. Antonov, I.S. Bonev, Chr.V. Christov, and I.Zh. Petkov, (1990) *Nuovo Cim.* **103A** 1287.

[25] M.V. Ivanov, A.N. Antonov, and M.K. Gaidarov, (2000) *Int. J. Mod. Phys.* **E9** No.4 339.

[26] M. Leuschner *et al.*, (1994) *Phys. Rev.* **C49** 955.

[27] D.J.S. Findlay and R.O. Owens, (1977) *Nucl. Phys.* **A279** 389.

[28] F. de Smet *et al.*, (1993) *Phys. Rev.* **C47** 652.

[29] G.J. Miller *et al.*, (1995) *Nucl. Phys.* **A586** 125.

[30] G. Benenti, C. Giusti, and F.D. Pacati, (1994) *Nucl. Phys.* **A574** 716.

[31] M. Anguiano, G. Co', A.M. Lallena, and S.R. Mokhtar, (2002) *Annals Phys.* **296** 235.

[32] C. Giusti, and F.D. Pacati, in preparation.

[33] G.S. Adams, E.R. Kinney, J.L. Matthews, W.W. Sapp, T. Soos, R.O. Owens, R.S. Turley, and G. Pignault, (1988) *Phys. Rev.* **C38** 2771.

[34] J.E. Amaro, A.M. Lallena, and J. A. Caballero, (1999) *Phys. Rev.* **C60** 014603.

[35] D. Van Neck, *et al.*, (1998) *Phys. Rev.* **C57** 2308.

[36] Y. Jin, D.S. Onley, and L.E. Wright, (1992) *Phys. Rev.* **C45** 1311;
Y. Jin, J.K. Zhang, D.S. Onley, and L.E. Wright, (1993) *Phys. Rev.* **C47** 2024;
Y. Jin and D.S. Onley, (1994) *Phys. Rev.* **C50** 377;
J.M. Udías *et al.*, (1993) *Phys. Rev.* **C48** 2731.

[37] S. Boffi, C. Giusti, F.D. Pacati, and F. Cannata, (1987) *Nuovo Cim.* **98** 291.

[38] A. Meucci, C. Giusti and F.D. Pacati, (2001) *Phys. Rev.* **C64** 014604.

[39] J. Gao *et al.*, (2000) *Phys. Rev. Lett.* **84** 3265.

[40] E.D. Cooper, S. Hama, B.C. Clark, and R.L. Mercer, (1993) *Phys. Rev.* **C47** 297.

[41] W. Pöschl, D. Vretenar, and P. Ring, (1997) *Comput. Phys. Commun.* **103** 217.

[42] A. Meucci, C. Giusti and F.D. Pacati, (2001) *Phys. Rev.* **C64** 064615.

[43] M.J. Leitch, J.L. Matthews, W.W. Sapp, C.P. Sargent, S.A. Wood, D.J.S. Findlay, R.O. Owens, and B.L. Roberts, (1985) *Phys. Rev.* **C31** 1633.

[44] T. de Forest, Jr., (1983) *Nucl. Phys.* **A392** 232.

[45] S. Pollock, H.W.L. Naus, and J.H. Koch, (1996) *Phys. Rev.* **C53** 2304.

[46] J.A. Caballero, T.W. Donnelly, E.Moya de Guerra, J.M. Udías, (1998) *Nucl. Phys.* **A632** 323.

[47] S. Jeschonnek and J.W. Van Orden, (2000) *Phys. Rev.* **C62** 044613.

[48] L.L. Foldy and S.A. Wouthuysen, (1950) *Phys. Rev.* **78** 29.

[49] C. Giusti and F.D. Pacati, (1980) *Nucl. Phys.* **A336** 427.

[50] A. Meucci, C. Giusti and F.D. Pacati, (2002) *Phys. Rev.* bf C66 034610.